Rapid Communications

Emergence of antiferromagnetic quantum domain walls

H. Y. Yuan,[1,*] Man-Hong Yung,[2,†] and X. R. Wang[3,4,‡]

[1]*Department of Physics, South University of Science and Technology of China, Shenzhen 518055, Guangdong, China*

[2]*Institute for Quantum Science and Engineering and Department of Physics, South University of Science and Technology of China, Shenzhen 518055, Guangdong, China*

[3]*Department of Physics, The Hong Kong University of Science and Technology, Clear Water Bay, Kowloon, Hong Kong, China*

[4]*HKUST Shenzhen Research Institute, Shenzhen 518057, China*

(Received 16 March 2018; revised manuscript received 2 August 2018; published 14 August 2018)

Domain walls (DWs), as interfaces separating different magnetic domains, are widely regarded as classical objects, even though the underlying constituents, namely, electron spins and spin-spin exchange interaction, are intrinsically of quantum nature. One intriguing question is, how do DWs behave when the size of the magnetic domains is shrunk to the atomistic level? Would quantum fluctuations destroy the stability of the DWs? These questions are partly addressed for ferromagnets, but seldom studied for antiferromagnets. Here we present a microscopic quantum spin model of antiferromagnets where the ground states not only share several common properties with the classical domain walls, but also exhibit nontrivial quantum properties. Specifically, the magnetization profile highly resembles its classical counterparts, even though the spins inside the domain walls are highly entangled. Furthermore, a nonzero spin angular momentum of a quantum DW emerges and it does not depend on the system size. Finally, we show that quantum DWs can be generated through a quantum phase transition from a quantum domain and the critical point can be characterized by the global entanglement. These results provide additional physical insights on the quantum effects in spintronics, and can be experimentally verified within the current technologies in superconducting circuits and trapped ions.

DOI: 10.1103/PhysRevB.98.060407

Introduction. In magnetic systems, spins can form various stable topologically nontrivial structures through an exchange interaction, such as domain walls (DWs) [1–3], vortices [4–7], and skyrmions [8–13]. At the macroscopic scale, it is often sufficient to approximate DWs as a classical object consisting of a collection of classical spin angular momentum [1,2]. This classical picture can be justified when the DW size is much wider than the exchange length [14,15]; in this way, the quantum fluctuations of spin orientations become negligible, and the average quantum spins follows the classical spin dynamics. Such a classical approximation is invalid as the DW size shrinks to the atomistic scale. To understand the physical behaviors of the DWs at the atomistic scale, a fully quantum-mechanical approach should be considered; this direction points to an overlapping area between the classical spintronics and quantum information science, which is largely unexplored.

At the atomistic scale, the states of quantum systems can be characterized by various quantum correlations, in particular, quantum entanglement [16,17], which can be regarded as a precious computation and information resource. So far, entangling tens of particles have been realized in experiments [18–26]. Furthermore, with the state-of-the-art technologies, such as those in superconducting circuits [18–20] and trapped ions [21–24], it is possible to control the spin-spin interaction from ferromagnetic to antiferromagnetic, and vice versa. These recent developments open intriguing possibilities for studying quantum properties of magnetic structures, such as DWs, vortices, and even skyrmions with a finite controllable number of spins in the laboratory. In this interdisciplinary area, there are many questions that remain unanswered, including the following: (i) In what physical systems does a quantum DW exist? (ii) What is the physical structure of the quantum DW? (iii) How can we detect the emergence of such quantum DW? These problems are partly studied in the anisotropic Heisenberg chain with ferromagnetic exchange interaction [27,28] and the phase transition in this model was mentioned in a follow-up work [29]. However, these questions are seldom studied in antiferromagnets that are fundamentally different from ferromagnets in quantum mechanics since one cannot map one to the other by a unitary transformation.

In this Rapid Communication, we focus on an antiferromagnetic quantum spin chain sandwiched between two magnetic domains, pinned at the boundary by strong fields. The ground state of the system defines a quantum DW, since the spatial variations of the expectation values of stagger magnetization are similar to those of its classical counterpart. Moreover, the spins inside the DW are highly entangled, while the average spin-spin entanglement naturally recovers the global entanglement of the quantum DW. Around the quantum transition point of DWs and domains, the scaling behavior of global entanglement suggests that it is a good indicator of phase transition.

Model of quantum DWs. Let us consider the Hamiltonian $\mathcal{H}$ of the transverse Ising model, where N spin-1/2 particles are

*yuanhy@sustc.edu.cn
†yung@sustc.edu.cn
‡phxwan@ust.hk

 ©2018 American Physical Society

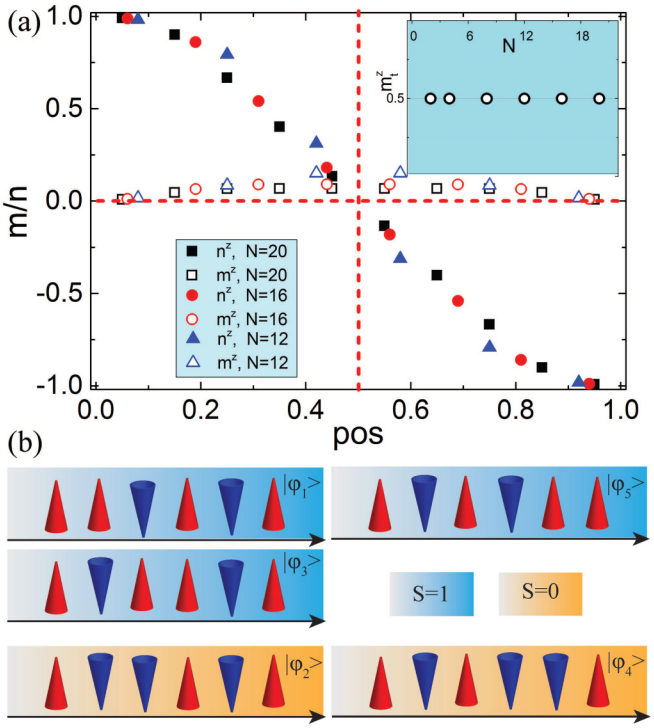

FIG. 1. (a) Spatial variation of m^z (open symbols) and n^z (filled symbols) for a spin chain with $N = 12$ (triangles), 16 (circles), and 20 (squares), respectively. The top-right inset shows the net magnetization as a function of N. pos $= i/N$ is the scaled position of the ith site, $g = 0.2$. (b) Scheme of the five degenerated low-energy excitation states for $N = 6$. The blue (orange) background represents the net magnetization of the corresponding state to be $S = 1$ ($S = 0$).

localized on a one-dimensional lattice, subject to the boundary fields h,

$$\mathcal{H} = J\sum_{\langle ij\rangle}\sigma_i^z\sigma_j^z - g\sum_{i=1}^{N}\sigma_i^x - h\left(\sigma_1^z + \sigma_N^z\right), \qquad (1)$$

where σ_i^x, σ_i^z are the Pauli matrices on the ith site, J is the exchange coupling, and g is the anisotropy constant. Here $\langle ij\rangle$ denotes nearest-neighbor spins. The ground-state energy E_0 and the corresponding ground state $|0\rangle$ is calculated using the standard Lancoz algorithm [30–32]. In the following, we shall focus on the antiferromagnetic (AFM) coupling ($J > 0$), but the results can be readily generalized to the ferromagnetic case as well. Here the magnetization m_i^z and staggered magnetization [33] n_i^z are given by

$$m_i^z = \tfrac{1}{2}\langle 0|\sigma_i^z + \sigma_{i+1}^z|0\rangle, \qquad n_i^z = \tfrac{1}{2}\langle 0|\sigma_i^z - \sigma_{i+1}^z|0\rangle, \quad (2)$$

where $i = 1, 3, 5, \ldots, N-1$.

Properties of quantum DWs. In the regime with weak anisotropy $g \ll J$, the profiles of the quantum DWs are similar to those of classical AFM DWs [see Fig. 1(a)]. (i) The staggered order n_z has a typical classical DW profile; it varies from 1 on the left-hand side of the chain to -1 on the right-hand side. (ii) The magnetization order m_z is zero near the boundary and reaches its maximum at the DW center. (iii) As the system becomes larger, the magnetic moments near the center become smaller, but, by summing all the magnetic moments in the DW, the total magnetic moment is numerically found to be a constant, i.e., $m_t^z = \sum_i m_i^z = 1/2$, independent of the system size N.

Proof of conserved total magnetic moment. In the following, we shall analytically prove the result of $m_t^z = 1/2$. Given the condition $g \ll J$, the AFM exchange interaction dominates the Hamiltonian (1). Thus, the lowest energy states include only one pair of neighboring spins aligned parallel [see Fig. 1(b)], while the other nearest-neighboring spins are antiparallel with each other. For example, for $N = 6$, there are five such configurations of same energy as sketched in Fig. 1(b). In general, there are $N-1$ such states of energy $-(N-3)J$. These states can be further classified into $|\varphi_i^{S=1}\rangle$ for $S = 1$ and $|\varphi_i^{S=0}\rangle$ for $S = 0$, $N/2$ for $S = 1$, and the remaining for $S = 0$, where S is the net magnetization of the system. The ground state under the boundary conditions is the linear combination of these states, $|0_{\rm th}\rangle = \sum_{i=1}^{N/2} a_i|\varphi_i^{S=1}\rangle + \sum_{i=1}^{N/2-1} b_i|\varphi_i^{S=0}\rangle$, where a_i, b_i are the superposition coefficients. By rearranging the basis states such that $S = 1$ and $S = 0$ states are ordered alternatively, the Hamiltonian (1) can be recast as a tridiagonal-Toeplitz matrix, where the ground-state energy is found to be $E_0 = -(N-3)J - 2g\cos(\pi/N)$, and $|0_{\rm th}\rangle = \sqrt{\frac{2}{N}}(\sin\frac{\pi}{N}, \sin\frac{2\pi}{N}, \ldots, \sin\frac{(N-1)\pi}{N})$ [34]. Note that the anisotropy term g only gives a first-order correction of the ground-state energy. As a result, the magnetic moments distribution is given by $m_i^z = \langle 0_{\rm th}|\sigma_i^z + \sigma_{i+1}^z|0_{\rm th}\rangle/2 = u_i$, where $u_i = 2/N\sin^2 i\pi/N$. The net magnetization can therefore be calculated as

$$m_t^z = \sum_{\text{odd } i}^{N-1} u_i = \frac{1}{2}, \qquad (3)$$

independent of N.

Purity of quantum DWs. In quantum information science, the purity of the ith spin is defined as $P_i = \mathrm{tr}(\rho_i^2)$ where ρ_i is the reduced density matrix of the ith spin; it takes the value 1 for a separable pure state, but $1/2$ for maximally entangled states such as Bell states and Greenberg-Horne-Zelinger states [35]. Furthermore, it can be experimentally measured [36] using standard techniques in quantum information science.

For the quantum DW, the purity of the ith spin is given by

$$P_i^{\rm th} = \left(\sum_{k=1}^{i-1} u_k\right)^2 + \left(\sum_{k=i}^{N-1} u_k\right)^2 + 2u_iu_{i-1}, \qquad (4)$$

where $i = 1, 2, \ldots, N$. The third term u_iu_{i-1} is of the order $O(1/N^2)$, which is much smaller than the first two terms. Considering $\sum u_i = 1$, P_i reaches its minimum value $(1/2)$ at $i = N/2$, i.e., the chain center, where $m_i^z = u_i \propto \sin^2(i\pi/N)$ reaches its maximum value.

Numerically, we found that the purity is close to 1 near the boundary of the spin chain and then decreases to form a symmetric dip around the chain center at $i/N = 1/2$, regardless of the system size [see Fig. 2(a)]. Moreover, the magnetization distribution of DWs takes on a peak centered at the dip position and its space dependence is strongly correlated with the purity. For the spins near the boundary, their directions are strongly bounded by the fixed orientations of the boundary

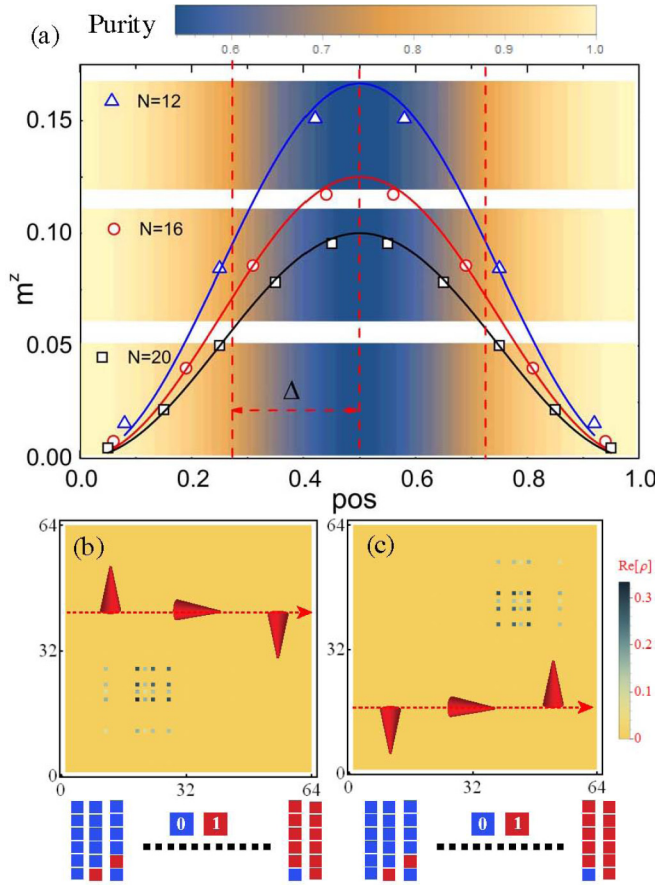

FIG. 2. (a) Distribution of the magnetic moments of DWs for $N = 12$ (triangles), 16 (circles), and 20 (squares), respectively. The solid lines are the theoretical results given by $m_i^z = u_i$. The colored strips represent the distribution of purity at the corresponding N. (b),(c) Density of states tomography for a clockwise/counterclockwise DW state in a spin chain with $N = 6$. The values of vertical/horizontal axis represents the value of the basis vector by treating up spin as bit 0 and down spin as bit 1. The inset sketches the DW profile.

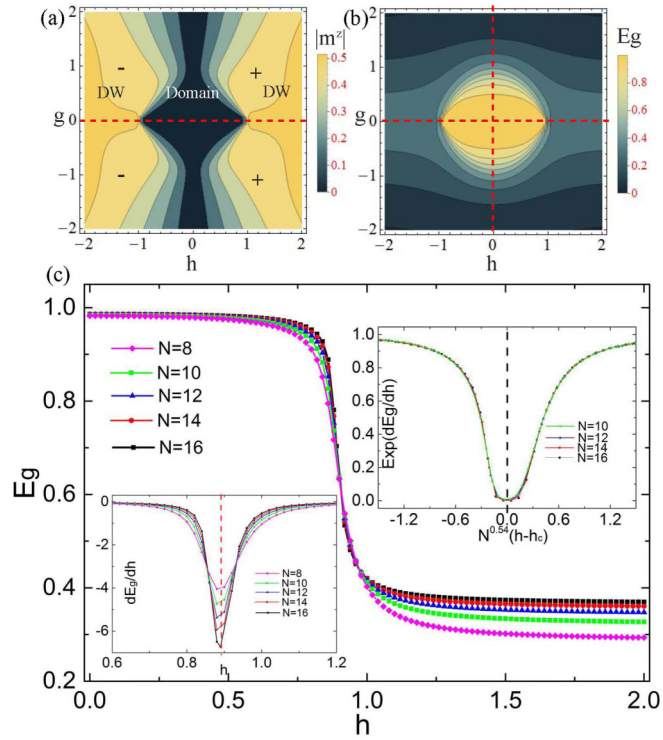

FIG. 3. (a) The distribution of net magnetization of the spin chain ($|m^z|$) in the h-g phase space. The $\pm$ signs represent clockwise and counterclockwise DWs, respectively. $N = 12$. (b) Simulated global entanglement (E_g) distribution in the h-g phase space. (c) Global entanglement (E_g) as a function of boundary field (h). $J = 1.0$, $g = 0.2$. Left inset: dE_g/dh as a function of external field for $N = 8, 10, 12, 14, 16$, respectively. Right inset: scaling behavior of the global entanglement around the critical point h_c.

spins and have a larger probability to be in Néel-state-like configurations. Consequently, the magnetization is close to zero and these spins are not entangled with the others (i.e., close to a pure state). The spins near the center are influenced lightly by the boundary spins and their directions become much more uncertain, hence the purity of these spins become smaller. The purity of spins is close to $1/2$ at the wire center, which suggests that the spins inside the DW are strongly entangled.

A typical tomography of the density matrix for a clockwise/counterclockwise DW is shown in Figs. 2(b) and 2(c). The distinguishable distributions of the density matrix allow us to classify clockwise and counterclockwise DWs in the atomistic scale.

Global entanglement of quantum DWs. Compared with classical DWs, the key distinctive feature of quantum DWs is that the local spins are highly entangled. In quantum information science, the *global entanglement*, E_g, of a pure quantum state can be quantified by the total purity [36,37]: $E_g \equiv \frac{2}{N}\sum_{i=1}^{N}(1 - P_i)$. To the leading order of $1/N$, the global entanglement can be determined by the following:

$$E_g = 2 - \frac{2}{N}\sum_{k=1}^{N}\left[\left(\sum_{i=1}^{k-1} u_i\right)^2 + \left(\sum_{i=k}^{N-1} u_i\right)^2\right]. \quad (5)$$

The sum increases as N increases and saturates numerically when $N > 20$. The limiting value for $N \gg 1$ is found to be $E_g = 2/3 - 5/2\pi^2 \approx 0.41$. This indicates that the spins in the quantum DW is still highly entangled in the macroscopic scale.

As an example, let us consider the case where $h = 0$ in the Hamiltonian $\mathcal{H}$; the ground state is a superposition of two degenerated Néel states,

$$|0_{\rm th}\rangle = \frac{1}{\sqrt{2}}(|\uparrow\downarrow\uparrow\downarrow\cdots\uparrow\downarrow\rangle + |\downarrow\uparrow\downarrow\uparrow\cdots\downarrow\uparrow\rangle), \quad (6)$$

which is referred to as the quantum domain state, as both magnetization and stagger order are zero. The global entanglement is $E_g = 1$, but its net magnetization is zero. Therefore, it becomes possible to distinguish quantum domain and quantum DW states by probing the global entanglement, which is analyzed qualitatively below.

Quantum phase transition. Here we consider the zero-temperature phase diagram of the quantum spin model; the exchange coupling J remains unchanged, but the anisotropy g and boundary fields h are varied (see Fig. 3). Guided by the red

line, we found that the ground state changes from the domain state to a quantum DW at the critical field of $h_c = J$ for $g = 0$.

The critical field has a nontrivial dependence on g and h. In the regime $g \ll 1$, the ground state depends on the competition of exchange interaction and Zeeman interaction. The global entanglement (E_g) drops abruptly from 1.0 to a small value, as shown in Fig. 3(c). Physically, when $h < h_c$, the exchange interaction dominates the Hamiltonian and the ground state is a superposition of two degenerated Néel states, Eq. (6), with $E_g = 1$. The numerical value of E_g is a little smaller than the theoretical value 1, as shown in Fig. 3(c), due to the small anisotropy g term, whose tendency is to align all the spins to the x direction and reduce the entanglement. As the field increases above h_c, the ground state becomes a DW state with a finite value of global entanglement.

Numerically, the global entanglement and its first derivative is continuous with h near the critical field, but its second-order derivative seems to be discontinuous, as shown in the left inset of Fig. 3(c). We shall show that discontinuity of the global entanglement is a good indicator of the phase transition. First, let us plot the first derivative of E_g versus h in the left inset of Fig. 3(c) for system size ranging from $N = 8, 10, 12, 14, 16$. As N increases, dE_g/dh shows a clear divergence tendency at the critical field.

To eliminate the finite-size effect, we perform a scaling analysis for finite systems using the scaling ansatz [38],

$$\frac{dE_g}{dh} = \ln N^{\nu}|h - h_c|, \tag{7}$$

where ν is the critical exponent. As shown in the right inset of Fig. 3(c), $\nu = 0.54$ gives perfect scaling results for the finite systems. These results suggest that global entanglement is a suitable measure of quantum DW/domain phase transition.

Discussions and conclusions. In this work, we have theoretically justified the existence of a quantum version of magnetic DWs, which has an intrinsic magnetization of 1/2 independent of size. The global entanglement of such a DW is nonzero and even exists at a macroscopic scale. Moreover, the magnetization profile is closely related to the local purity of spins, where the DW width can be extracted from the purity profile and experimentally verified. Specifically, the typical energy gap of the ground state and first excited state in our model is 44 μeV ($\sim$528 mK) for $N = 20$ ($J = 10$ meV and $g = 0.6$ meV) [39]. Then the mixture of excited states and ground state can be neglected at a temperature below 527 mK, which leaves sufficient room to experimentally verify our theoretical prediction in platforms working in low temperature. Alternatively, it is promising to test our prediction of quantum DWs in a trapped ions system, where the transverse Ising model with tunable spin-spin coupling has been realized [24,40].

Secondly, the stability of quantum DWs may be influenced by temperature-induced decoherence, defects, field gradients, and dipolar interaction. (1) We estimate [41–43] the occupation probability of the excited states, i.e., $P = 1 - \exp(-E_0/k_BT)/Z \sim 5 \times 10^{-5}$, where k_B is the Boltzmann constant and Z is the partition function of the system at $T = 53$ mK. Therefore, the decoherence should be considerably slow at low temperature. (2) The random defects and field gradient cannot demolish the quantum DWs if their effective strength is far from the phase boundary shown in Fig. 3(a) [44–46]. One interesting observation is that the quantum DW center shifts under a field gradient, which may lead to DW motion under inhomogeneous field [33]. (3) The influence of dipolar interaction on the antiferromagnetic DW is negligible due to the cancellable response of the internal sublattices. This is widely viewed as an advantage of antiferromagnets over ferromagnets [47].

Finally, our results are applicable to chiral DWs due to competition between the Dzyaloshinskii-Moriya interaction (DMI) [48–50] and the normal exchange interaction. By generalizing our conclusions to two dimensions, the magnetic quantum skyrmion is expected to exist. This type of skyrmion has nonzero entanglement that is different from the classical skyrmions. A promising platform to observe this chiral structure is a superconducting circuit, where the effective DMI has been synthesized in a 5-qubit system [51].

Acknowledgments. H.Y.Y. acknowledges financial support from National Natural Science Foundation of China (NSFC) (Grant No. 61704071). M.H.Y. acknowledges support from NSFC (Grant No. 11405093), Guangdong Innovative and Entrepreneurial Research Team Program (2016ZT06D348), Natural Science Foundation of Guangdong Province (Grant No. 2017B030308003), and Science, Technology and Innovation Commission of Shenzhen Municipality (Grants No. ZDSYS20170303165926217 and No. JCYJ20170412152620376). X.R.W. was supported by the NSFC (Grants No. 11374249 and No. 11774296) as well as Hong Kong RGC (Grants No. 16301518 and No. 16301816).

[1] A. Hubert and R. Schäfer, *Magnetic Domains: The analysis of Magnetic Microstructures* (Springer, Berlin/Heidelberg, 1998).
[2] H. Y. Yuan and X. R. Wang, Phys. Rev. B **92**, 054419 (2015).
[3] H. Y. Yuan, Z. Yuan, K. Xia, and X. R. Wang, Phys. Rev. B **94**, 064415 (2016).
[4] T. Shinjo, T. Okuno, R. Hassdorf, K. Shigeto, and T. Ono, Science **289**, 930 (2000).
[5] A. Wachowiak, J. Wiebe, M. Bode, O. Pietzsch, M. Morgenstern, and R. Wiesendanger, Science **298**, 577 (2002).
[6] S.-B. Choe, Y. Acremann, A. Scholl, A. Bauer, A. Doran, J. Stöhr, and H. A. Padmore, Science **304**, 420 (2004).
[7] H. Y. Yuan and X. R. Wang, AIP Adv. **5**, 117104 (2015).
[8] A. N. Bogdanov and U. K. Rößler, Phys. Rev. Lett. **87**, 037203 (2001).
[9] U. K. Rößler, A. N. Bogdanov, and C. Pfleiderer, Nature (London) **442**, 797 (2006).
[10] S. Mühlbauer, B. Binz, F. Jonietz, C. Pfleiderer, A. Rosch, A. Neubauer, R. Georgii, and P. Böni, Science **323**, 915 (2009).
[11] X. Z. Yu, Y. Onose, N. Kanazawa, J. H. Park, J. H. Han, Y. Matsui, N. Nagaosa, and Y. Tokura, Nature (London) **465**, 901 (2010).
[12] H. Y. Yuan and X. R. Wang, Sci. Rep. **6**, 22638 (2016).
[13] H. Y. Yuan, O. Gomonay, and M. Kläui, Phys. Rev. B **96**, 134415 (2017).

[14] J. E. Miltat and M. J. Donahue, *Numerical Microsmagnetics: Finite Difference Methods in the Book Handbook of Magnetism and Advanced Magnetic Materials* (Wiley, New York, 2007).

[15] H. Y. Yuan and X. R. Wang, J. Magn. Magn. Mater. **368**, 70 (2014).

[16] M. A. Nielsen and I. L. Chuang, *Quantum Computation and Quantum Information*, 10th Anniversary ed. (Cambridge University Press, Cambridge, UK, 2000).

[17] H. Y. Yuan and M.-H. Yung, Phys. Rev. B **97**, 060405(R) (2018).

[18] M. Neeley, R. C. Bialczak, M. Lenander, E. Lucero, M. Mariantoni, A. D. O'Connell, D. Sank, H. Wang, M. Weides, J. Wenner, Y. Yin, T. Yamamoto, A. N. Cleland, and J. M. Martinis, Nature (London) **467**, 570 (2010).

[19] L. Dicarlo, M. D. Reed, L. Sun, B. R. Johnson, J. M. Chow, J. M. Gambetta, L. Frunzio, S. M. Girvin, M. H. Devoret, and R. J. Schoelkopf, Nature (London) **467**, 574 (2010).

[20] C. Song, K. Xu, W. Liu, C. P. Yang, S. B. Zheng, H. Deng, Q. Xie, K. Huang, Q. Guo, L. Zhang, P. Zhang, D. Xu, D. Zheng, X. Zhu, H. Wang, Y. A. Chen, C. Y. Lu, S. Han, and J.-W. Pan, Phys. Rev. Lett. **119**, 180511 (2017).

[21] B. Lanyon, C. Hempel, D. Nigg, M. Müller, R. Gerritsma, F. Zähringer, P. Schindler, J. T. Barreiro, M. Rambach, G. Kirchmair, M. Hennrich, P. Zoller, R. Blatt, and C. F. Roos, Science **334**, 57 (2011).

[22] P. Jurcevic, B. P. Lanyon, P. Hauke, C. Hempel, P. Zoller, R. Blatt, and C. F. Roos, Nature (London) **511**, 202 (2014).

[23] J. Zhang, G. Pagano, P. W. Hess, A. Kyprianidis, P. Becker, H. Kaplan, A. V. Gorshkov, Z.-X. Gong, and C. Monroe, Nature (London) **551**, 601 (2017).

[24] P. Jurcevic, H. Shen, P. Hauke, C. Maier, T. Brydges, C. Hempel, B. P. Lanyon, M. Heyl, R. Blatt, and C. F. Roos, Phys. Rev. Lett. **119**, 080501 (2017).

[25] R. Barends, J. Kelly, A. Megrant, A. Veitia, D. Sank, E. Jeffrey, T. C. White, J. Mutus, A. G. Fowler, B. Campbell, Y. Chen, Z. Chen, B. Chiaro, A. Dunsworth, C. Neill, P. O'Malley, P. Roushan, A. Vainsencher, J. Wenner, A. N. Korotkov, A. N. Cleland, and J. M. Martinis, Nature (London) **508**, 500 (2014).

[26] H. Bernien, S. Schwartz, A. Keesling, H. Levine, A. Omran, H. Pichler, S. Choi, A. S. Zibrov, M. Endres, M. Greiner, V. Vuletić, and M. D. Lukin, Nature (London) **551**, 579 (2017).

[27] R. Schilling, Phys. Rev. B **15**, 2700 (1977).

[28] F. C. Alcaraz, S. R. Salinas, and W. F. Wreszinski, Phys. Rev. Lett. **75**, 930 (1995).

[29] F. C. Alcaraz, A. Saguia, and M. S. Sarandy, Phys. Rev. A **70**, 032333 (2004).

[30] C. Lanczos, J. Res. Natl. Bur. Stand. **45**, 255 (1950).

[31] E. Dagotto, Rev. Mod. Phys. **66**, 763 (1994).

[32] See Supplemental Material at http://link.aps.org/supplemental/10.1103/PhysRevB.98.060407 for simulation details.

[33] H. Y. Yuan, W. Wang, M.-H. Yung, and X. R. Wang, Phys. Rev. B **97**, 214434 (2018).

[34] See Supplemental Material at http://link.aps.org/supplemental/10.1103/PhysRevB.98.060407 for the detailed derivation.

[35] D. M. Greenberger, M. A. Horne, and A. Zeilinger, arXiv:0712.0921.

[36] G. K. Brennen, Quantum Inf. Comput. **3**, 616 (2003).

[37] D. A. Meyer and N. R. Wallach, J. Math. Phys. **43**, 4273 (2002).

[38] A. Osterloh, L. Amico, G. Falci, and R. Fazio, Nature (London) **416**, 608 (2002).

[39] The energy gap of the first excited state and the ground state is $\Delta E = E_1 - E_0 = 2|g|(\cos\frac{\pi}{N} - \cos\frac{2\pi}{N}) = 44\ \mu\text{eV} \sim 528$ mK, where $J = 10$ meV corresponds to 120 K.

[40] K. Kim, M.-S. Chang, R. Islam, S. Korenblit, L.-M. Duan, and C. Monroe, Phys. Rev. Lett. **103**, 120502 (2009).

[41] The analytical treatment of the decoherence for a two and more qubits system is almost impossible and the numerical integration of the Schrödinger equation is often used to obtain the time dependence of the density matrix of the system [42]. Here the global entanglement introduced by Meyer and Wallach fails for this thermal state and it is still a challenge to find a well justified and easily tractable measure to quantify the global entanglement of a multispin system [43], which is beyond the scope of current work. This is why we take an alternate to estimate the energy gap.

[42] S. Yuan, J. Comput. Theor. Nanosci. **8**, 889 (2011).

[43] P. J. Love, A. Maassen van den Brink, A. Yu. M. H. Smirnov, S. Amin, M. Grajcar, E. Il'ichev, A. Izmalkov, and A. M. Zagoskin, Quantum Inf. Process. **6**, 187 (2007).

[44] See Supplemental Material at http://link.aps.org/supplemental/10.1103/PhysRevB.98.060407 for detailed modeling and discussion of the effects of defects and field gradient on the stability of quantum domain walls.

[45] J. Leliaert, B. Van de Wiele, A. Vansteenkiste, L. Laurson, G. Durin, L. Dupré, and B. Van Waeyenberge, Phys. Rev. B **89**, 064419 (2014).

[46] T. J. G. Apollaro and F. Plastina, Phys. Rev. A **74**, 062316 (2006).

[47] T. Jungwirth, X. Marti, P. Wadley, and J. Wunderlich, Nat. Nanotechnol. **11**, 231 (2016).

[48] I. E. Dzyaloshinskii, Sov. Phys. JETP **5**, 1259 (1957).

[49] T. Moriya, Phys. Rev. **120**, 91 (1960).

[50] See Supplemental Material at http://link.aps.org/supplemental/10.1103/PhysRevB.98.060407 for the analytical solution of the ground state with DMI included.

[51] D.-W. Wang, C. Song, W. Feng, H. Cai, D. Xu, H. Deng, D. Zheng, X. Zhu, H. Wang, S. Zhu, and M. O. Scully, arXiv:1712.05261.